ACTA METALLURGICA SLOVACA
2021, VOL. 27, NO. 3, 127-132

RESEARCH PAPER

EFFECT OF COOLING RATE ON MICROSTRUCTURE AND HARDNESS IN GRAY CAST IRON CASTING PROCESS

Agus Yulianto[1, 2], Rudy Soenoko[2], Wahyono Suprapto[2], As'ad Sonief[2]

[1] Department of Mechanical Engineering, Faculty of Engineering, Universitas Muhammadiyah Surakarta, Indonesia

[2] Department of Mechanical Engineering, Faculty of Engineering, Brawijaya University, Indonesia

* Corresponding author: ay160@ums.ac.id, tel.: Faculty of Engineering / Universitas Muhammadiyah Surakarta, 57162, Surakarta, Indonesia

Received: 31.05.2021
Accepted: 24.08.2021

ABSTRACT

Casting is conducted by melting and solidifying the metal and forming it according to the desired shape in the mold. Due to environmental issues, there were considerations to choose permanent molds instead of sand molds. This study aims to investigate the thermal conditions of the molds, changes in microstructure and hardness of casting products using sand mold and permanent mold. The use of sand mold and permanent mold results in different cooling rates. Thermal analysis was performed using a thermocouple to obtain a temperature versus time curve. Metallographic observations were carried out using a Scanning Electron Microscope equipped with Energy-Dispersive X-ray Spectroscopy. The Vickers hardness test was carried out in three areas with different thicknesses. The results showed a constant temperature at 691 °C where the eutectoid phase reaction occurred. Testing with sand mold showed that cast iron with flake graphite was finer and spreader than graphite in cast iron produced by permanent mold. Meanwhile, gray cast iron from a casting process with a permanent mold has a higher hardness than gray cast iron from a casting process using a sand mold.

Keywords: cooling rate; graphite; gray cast iron; hardness

INTRODUCTION

Metal casting is the process of pouring molten metal into a mold for the manufacture of a variety of components, from high-performance automotive components to household goods. This casting process is widely used because it is relatively simple and can be used to make components with complex shapes, for example, objects that have internal channels and cavities [1, 2]. The casting process is not only used for cast iron, but also for non-ferrous materials [3-7].

Gray cast iron has flake -shaped graphite, while ductile cast iron has nodular graphite [8]. The formation of graphite is influenced by silicon; the more silicon the more graphite is formed [9]. It is generally accepted that flake graphite is formed in cast iron with high concentrations of oxygen and sulfur. Meanwhile, nodular graphite is formed in cast iron with low oxygen and sulfur content [10].

Mold plays an important role in the casting process. Research on mold has been done a lot. Jafar and Behnam [11] investigated the effect of mold preheating and ductile cast iron silicon composition on number of graphite nodules, carbide percentage and shrinkage volume. The results showed that when the preheating of the mold was increased, the carbide percentage and shrinkage volume decreased. Ductile cast iron with a carbon equivalent of 4.45% and a silicon composition of 2.5% without porosity defects is achieved when preheating of the mold is 450 °C. Increasing the silicon composition in the range of 2.1% -3. 3% causes an increase in the number of graphite nodules and the size of the graphite and a decrease in the percentage of carbides. This is due to the increase in expansion pressure induced during the formation of graphite with an increase in the silicon composition. Suitable conditions for casting sound products from ductile iron without riser at a mold preheating temperature of 300 °C are a carbon equivalent of 4.7% and a silicon composition of 3.3%.

Mold for the casting process can be disposable or permanent. An example for a single-use mold is a sand mold, while an example for a permanent mold is a metal mold. Behnam et al. [12] studied the microstructural and mechanical properties involving gray cast iron using sand molds. The effect of cooling rate on primary dendrite arm spacing (DAS), secondary dendrite arm spacing (SDAS), ferrite-cementite layer thickness and hardness (HB) were evaluated. The results show that DAS and SDAS as well as the thickness of the ferrite-cementite layer are highly dependent on the cooling rate, and they decrease as the cooling rate increases. The results also showed that the hardness increased with decreasing DAS, SDAS and the thickness of the ferrite-cementite layer.

Lerner [13] provided information that cast iron casting using Permanent Mold (PM) is almost 15% developed by the countries of the former Soviet Union, Germany, Eastern Europe and Japan, a small part in the United States and Canada, and several Asian countries. Although cast iron casting using PM technology originated in the US, it was also noted that the process has been widely used overseas. In Europe, 6-8% of all iron foundries are made with PM. Increasing use of the PM is also occurred in China and India.

As per statistical data, mold making, core, and smelting operations account for nearly 27% of the total energy costs in casting.

This will be much less in the case of the PM process. The problems that have been mentioned encourage casting stakeholders around the world to seriously consider the possibility and feasibility of replacing sand casting to PM casting. It is highly recommended that for Green Foundry [14]. Foundry not only requires the best technology, but also must meet environmentally friendly requirements [15].
Foundry using Permanent Mold is currently widely used to produce components in various industrial sectors, especially automobile power train components, including engine blocks and related components such as cylinder heads, and many other parts that require high mechanical properties [16].
Measurement of cooling rate in casting using PM for iron alloys is somewhat limited. There is also very little published literature on this topic. The subject is discussed in some publication literature sometimes, covers only some very general aspects. This clearly shows that the technology is not yet popular [17]. However, several investigators have investigated the effect of cooling rate on the casting process, in both ferrous and non-ferrous alloy castings.
In this research, the investigation was carried out with the aim of analyzing the thermal conditions, microstructure changes and hardness of ductile cast iron. Casting is conducted using a sand mold and a permanent mold which have different cooling rates. This research contributed to providing curves of cooling rate, microstructures evolution and hardnesses in sand and permanent mold castings.

MATERIAL AND METHODS

There were two types of molds used in the casting process. The first was permanent mold. Permanent mold was made of ferro cast ductile (FCD). FCD is a type of cast iron with a carbon content above 2.06%, has pearlite phase and/or ferrite phase as a matrix and contains nodular graphite [23]. The second was sand mold. The green-sand used in this research contained silica sand, bentonite 7.5% – 9%, water 3.5% – 4.5% and coal-dust. The green sand had the characteristics of easy disassembly and excellent recycling ability.
In this research, the FC 25 class gray cast iron was used with a chemical composition which can be seen in **Table 1**. The specimens of the smelting of gray cast iron or Chill Test (CT) were used to make small casts with a diameter of 30 mm and a thickness of 20 mm. The CT was poured before the liquid was poured onto the V-block specimen in permanent mold and sand molds. Prior to spectrometer processing, the CT specimen was cleaned with acetone and shot with argon gas.

Table 1 Chemical composition of gray cast iron (FC 25)

C (%)	Si (%)	Mn (%)	P (%)	S (%)	Cu (%)	Sn (%)	Mg (%)	Cr (%)	Ni (%)	Al (%)	Mo (%)
3,35	2,47	0,72	0,06	0,01	0,04	0,01	0,04	0,08	0,05	0,01	0,01

The cooling rate research was carried out using the V block shape mold from metal (FCD) and sand. Measurement of cooling temperature with a thermocouple attached to 3 points of the printed wall which was connected and recorded on the data logger using a computer-based system with the PLX-DAQ Release 2.0 data recorder (**Fig. 1**). Data were in the form of temperature in Excel software. The detailed data was then processed into a Temperature and Time (T-t) graph.

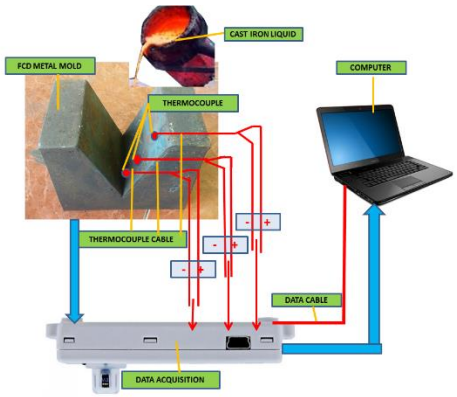

Fig. 1 The circuit for recording temperature data from thermocouple to computer

Microstructure investigations were carried out using a Scanning Electron Microscope (SEM). SEM is a type of electron microscope that produces an image of a sample by scanning a surface with a focused electron beam at a magnification up to a certain scale. The electrons interact with the atoms in the sample, producing various signals that contain information about the surface topography and composition of the sample. The SEM used in this study was the Quanta X50 SEM Series.

Energy Dispersive X-Ray (EDX) was installed on SEM and used for elemental chemical analysis of materials. This characterization ability is due in large part to the basic principle that each element has a unique atomic structure which allows a unique set of peaks on its electromagnetic emission spectrum (which is the main principle of spectroscopy).
The hardness test was carried out using the Vickers micro technique. This test based on ASTM E384 Standard. The Vickers hardness number was based upon the force divided by the surface area of the indentation. The load of 100 gf was applied to the specimens. The test location was divided into 3 points, namely points 1, 2 and 3 as shown in **Fig. 2**.

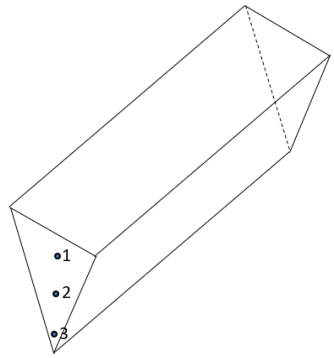

Fig. 2 Location of hardness test

RESULTS AND DISCUSSION

Thermal Investigations

The curves of the relationship between temperature and time in the permanent mold and sand mold as measured by a thermocouple are shown in the **Fig. 3**. The temperature vs time curves

are then attached to the Fe-C phase equilibrium diagram (**Fig. 4**).

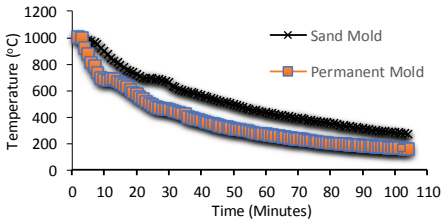

Fig. 3 Curves of solidification process in terms of temperature vs time on permanent mold and sand mold

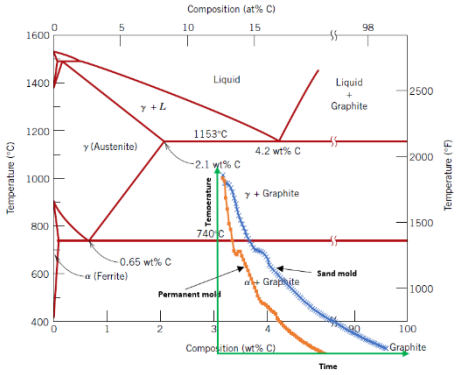

Fig. 4 The temperature vs time curve is attached to the Fe-C phase equilibrium diagram

A phase diagram is a diagram illustrating the relationship between temperature and composition in which a phase change occurs during slow cooling and heating processes. If iron is alloyed with carbon, the transformation that occurs over a certain temperature range is closely related to the carbon composition. The diagram of the cooling or solidification process of gray cast iron that has been obtained from the permanent mold and sand mold (Fig. 3) is connected to the temperature at which solidification occurs and is attached to the cast iron area in the phase diagram above 2% C (Fig. 4). The phase diagram shows the relationship between temperature and carbon composition, while the cooling/solidification process diagram shows the relationship between temperature and time. So that it will be known the gradient of the cooling rate of gray cast iron with permanent molds and sand molds and it is known that the phase is in the area above 2% C and below 1023 °C.

Table 2 Cooling rate of solidification in permanent mold and sand mold.

Mold Type	Cooling Rate (°C/min)
Permanent Mold	13.3
Sand Mold	7.3

At a temperature of 1023 °C, gray cast iron started to solidify. The cooling rate in permanent molds is faster than in the sand mold. In permanent molds, it passed a temperature of 691 °C in 18 minutes, while sand molds take 30 minutes. The cooling rate in the casting process with permanent mold and sand mold is approximated by calculating the slope of the curve. The results are shown in **Table 2**.

Metallography Investigations

Solidification in this study was recorded starting at a temperature of 1023 °C. The phases that occur at this temperature are the austenite and ledeburite phases. When the temperature reaches a constant eutectoid temperature of 691 °C, a eutectoid phase reaction occurs where the proeutectic austenite phase (austenite formed before the eutectic phase reaction) and austenite from ledeburite transforms into eutectoid ferrite and eutectoid cementite (pearlite) [24]. However, some of the cementite in pearlite will decompose into ferrite and graphite. The resulting ferrite will mix with cementite to form pearlite. When the temperature then decreases to room temperature, there is no significant phase change. Hence in the end it will form ferrite, pearlite and graphite phases at room temperature. **Fig. 5** shows the graphite phase (black color) with a pearlite (gray color) and ferrite (white color) matrix. In sand mold casting, fine graphite is seen dispersed in the pearlite and ferrite matrix. Meanwhile, in the permanent mold casting, the graphite appears larger than in the sand mold casting. But pearlite in casting with permanent mold looks more.

The size and amount of graphite in cast iron are influenced by the carbon content, the amount of added graphite and the choice of inoculation practice [25]. In addition, the silicon content in cast iron will inhibit the formation of cementite during the solidification process and facilitate the formation of graphite [26]. Graphite that is formed in casting with sand mold is rose-shaped and the fine flakes spread. The figure shows that the permanent mold will produce graphite in the form of flakes that is bigger than the graphite produced from the casting process with a sand mold.

The results of the composition test using Energy-dispersive X-ray spectroscopy are shown in **Fig. 6**. Silicon is present in the composition of 2.94 wt. % (4.11 at %). Silicon has the function of inhibiting C from reacting with Fe to form Fe3C so that C will be present as free carbon (graphite).

Hardness Investigations

The hardness test was carried out using the Vickers Micro hardness tester, the test results can be seen in Table 3 and Fig. 7. Casting using a permanent mold produces hardness at the bottom, middle and top locations of 256.30 VHN, 247.79 VHN and 228.57 VHN, respectively. While casting with sand mold produces hardness at bottom, middle and top locations of 168.85 VHN, 132.60 VHN and 123.83 VHN, respectively.

Fig. 7 shows that casting using a permanent mold produces a higher hardness than using a sand mold. This is because casting with permanent mold produces more pearlite phase than pearlite phase in sand mold casting. Pearlite is harder than ferrite because it contains hard cementite. Cementite is hard because cementite is a compound between iron and carbon which has ionic bonds. The unit cell of cementite is orthorhombic. While ferrite is a solid solution that has a metal bond with a body centered cubic (BCC) unit cell.

Fig. 7 also shows that the highest hardness of the casting with permanent mold of 256.30 VHN was obtained at the bottom location. This hardness is higher than the highest hardness in casting with sand mold of 168.85 VHN. This is caused by the cooling rate of casting with permanent mold is higher than with sand mold so that more pearlite is formed due to reduced decomposition of cementite into ferrite and graphite.

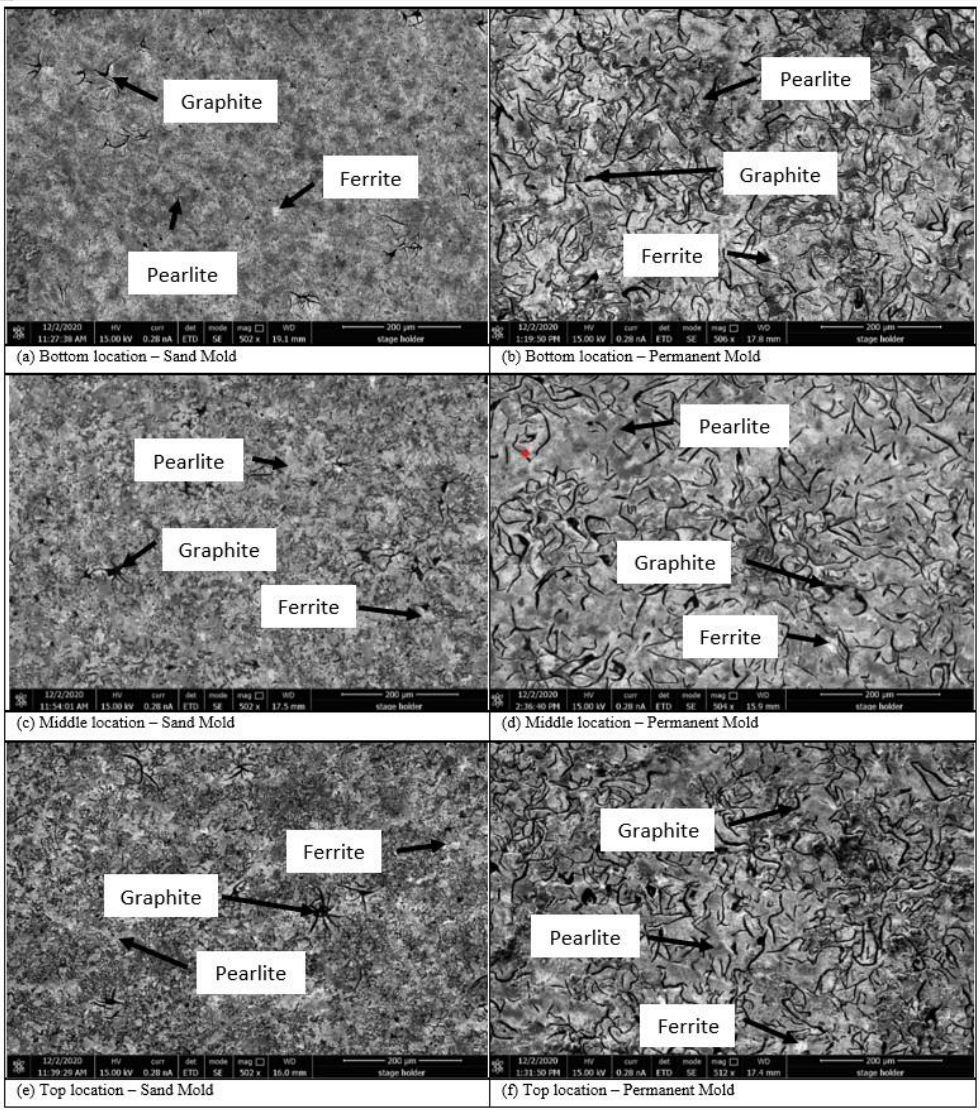

Fig. 5 Gray Cast Iron microstructure casted with sand mold and permanent mold

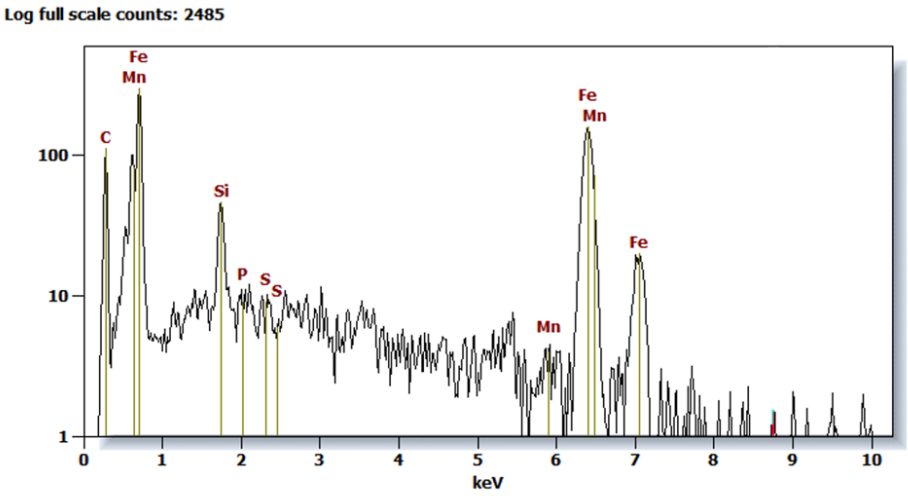

Element	Net Counts	Int. Cps/nA	Weight %	Atom %
C	521	14.472	10.74	35.05
Si	340	9.444	2.94	4.11
P	20	0.556	0.15	0.19
S	41	1.139	0.30	0.37
Mn	22	0.611	0.67	0.48
Fe	2482	68.944	85.19	59.80
		Total	100.00	100.00

Fig. 6 Composition test results using Energy-dispersive X-ray spectroscopy

Table 3 Hardness test result

Mold	Location	Vickers Hardness Number (VHN)	Average Vickers Hardness Number (VHN)
Permanent Mold	Top (location 1)	229.61	228.57
		229.08	
		227.03	
	Middle (location 2)	248.64	247.79
		246.01	
		248.71	
	Bottom (location 3)	256.94	256.30
		256.84	
		255.11	
Sand Mold	Top (location 1)	123.49	123.83
		123.22	
		124.77	
	Middle (location 2)	133.70	132.60
		132.44	
		131.66	
	Bottom (location 3)	169.34	168.85

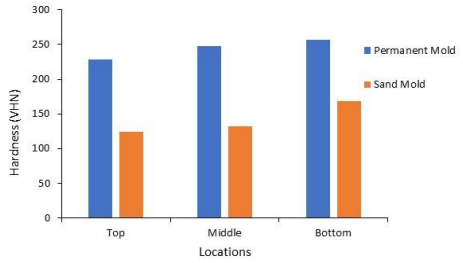

Fig. 7 Hardness test result

CONCLUSION

From the data generated during the study, it can be concluded that:

1. The eutectoid reaction is predicted to occur at a constant temperature of 691 °C
2. The phase formed in gray cast iron is flake graphite with pearlite matrix
3. Casting with permanent mold produces gray cast iron with a higher hardness than casting using sand mold. The thickness of the product has an effect on hardness, the thicker the product, the less hardness it is.

ACKNOWLEDGMENTS

The author would like to thank the Mechanical Laboratory, Department of Mechanical Engineering, Universitas Muhammadiyah Surakarta for facilitating the mechanical testing of gray cast iron, the author also thanks the CAD/CAM/CAE laboratory, Faculty of Engineering, Universitas Muhammadiyah Surakarta for facilitating the thermal simulation process.

REFERENCES

1. A. S. Darmawan, P. I. Purboputro, A. Yulianto, A. D. Anggono, Wijianto, Masyrukan, R. D. Setiawan, N. D. Kartika: Materials Science Forum, 991, 2020, 17-23. https://doi.org/10.4028/www.scientific.net/MSF.991.17.
2. G. d. M. Stieven, D. d. R. Soares, E. P. Oliveir, E. F. Lins: International Journal of Heat and Mass Transfer, 166, 2021, 120765. https://doi.org/10.1016/j.ijheatmasstransfer.2020.120765.
3. M. M. J. Behnam, P. Davami, N. Varahram: Materials Science and Engineering: A, 528(2), 2010, 583–588. https://doi.org/10.1016/j.msea.2010.09.087.
4. J. P. Weiler: Journal of Magnesium and Alloys, 9, 2020, 102–111. https://doi.org/10.1016/j.jma.2020.05.008.
5. L. D. Setyana, M. Mahardika, Suyitno: Acta Metallurgica Slovaca, 26(3), 2020, 132-137. https://doi.org/10.36547/ams.26.3.535.
6. H. A. Elamami, A. Incesu, K. Korgiopoulos, M. Pekguleryuz, A. Gungor: Journal of Alloys and Compounds, 764, 2018, 216-225. https://doi.org/10.1016/j.jallcom.2018.05.309.
7. K. V. Shankar, R. Sambhu, E. P. Sreedev: Materials Today: Proceedings, 24, 2020, 167-176. https://doi.org/10.1016/j.matpr.2020.04.264.
8. E. L. Neacsu, I. Riposan, A. M. Cojocaru, S. Stan, I. Stan: Metals, 10(8), 2020, 993. https://doi.org/10.3390/met10080993.
9. I. Stan, D. Anca, S. Stan, I. Riposan: Metals, 11(5), 2021, 846. https://doi.org/10.3390/met11050846.
10. H. M. Muhmond, H. Fredriksson: Metallurgical and Materials Transactions A, 45(13), 2014, 6187–6199. https://doi.org/10.1007/s11661-014-2589-2.
11. T. D. A. Jones, R. I. Strachan, D. M. Mackie, M. Cooper, B. Frame, J. B. Vorstius. Engineering Science and Technology, an International Journal, 24(1), 2021, 92-104. https://doi.org/10.1016/j.jestch.2020.12.009.
12. K. A. Jafar, A. A. Behnam: Journal of Iron and Steel Research, International, 18(3), 2011, 34–39. https://doi.org/10.1016/s1006-706x(11)60034-4.
13. [5/24/2021], https://www.thefreelibrary.com/Another+approach+to+iron+casting%3A+the+permanent+mold+process.-a019043902.
14. M. Holmgren, P. Nayström: The Green Foundry. In.: *the 68th World Foundry Congress*, Chennai, WFO, 2008, p. 15-17
15. S. Saetta, V. Caldarelli: Procedia Manufacturing, 42, 2020, 498–502. https://doi.org/10.1016/j.promfg.2020.02.042.
16. A. Hamasaiid, M. S. Dargusch, G. Dour: Journal of Manufacturing Processes, 47, 2019, 229–237. https://doi.org/10.1016/j.jmapro.2019.09.039.
17. M. S. Ramaprasad, M. N. Srinivasan: Permanent Molding of Cast Irons – Present Status and Scope. In.: *Science and Technology of Casting Processes*, edited by M. N. Srinivasan, Rijeka: InTech, 2012, p. 117-168. http://dx.doi.org/10.5772/50730.
18. F. F. O. Lima, L. F. Bauri, H. B. Pereira, C. R. Azevedo: International Journal of Cast Metals Research, 33(4-5), 2020, 1-17. https://doi.org/10.1080/13640461.2020.1822573.
19. B. Bauer, I. M. Pokopec, M. Petrič P. Mrvar: International Journal of Metalcasting, 14, 2020, 809-815. https://doi.org/10.1007/s40962-020-00432-3.
20. Z. Sun: Journal of Mechanical Engineering, 53(22), 2017, 67. https://doi.org/10.3901/JME.2017.22.067.
21. G. Liang, Y. Ali, G. You, M.-X. Zhang: Materialia, 3, 2018, 113-121. https://doi.org/10.1016/j.mtla.2018.08.008.
22. D. Chemezov, L. Smirnova, E. Bogomolova: International Scientific Journal Theoretical & Applied Science, 61(5), 2018, 132-14. https://doi.org/10.15863/TAS.
23. A. S. Darmawan, A. Yulianto, Masyrukan, P. I. Purboputro, G. N. Jati: International Journal of Emerging Trends in Engineering Research, 8(6), 2020, 2365-2369. https://doi.org/10.30534/ijeter/2020/26862020.
24. W. D. Callister, Jr., D. G. Rethwisch: *Materials Science and Engineering An Introduction*, 9th Edition, Hoboken: John Wiley & Sons, Inc, 2014
25. E. E. T. ELSawy, M. R. EL-Hebeary, I. S. E. El Mahallawi: Wear, 390-391, 2017, 113-124. https://doi.org/10.1016/j.wear.2017.07.007.
26. A. Yulianto, R. Soenoko, W. Suprapto, A. Sonief, A. S. Darmawan: International Journal of Emerging Trends in Engineering Research, 8(3), 2020, 617-622. https://doi.org/10.30534/ijeter/2020/02832020.